A GENUINELY MULTIDISCIPLINARY JOURNAL

CHEM**PLUS**CHEM

CENTERING ON CHEMISTRY

Accepted Article

Authors: Satyawan Nagane; Amol Ichake; Ishita Agrawal; Aditya Sadhanala; Richard Friend; Satishchandra Ogale; Prakash P. Wadgaonkar

A Journal of

ChemPubSoc
Europe

WILEY-VCH

www.chempluschem.org

Phenothiazine-Based D-A-π-A Dyes for Highly Efficient Dye Sensitized Solar Cells: Effect of Internal Acceptor and Non-Conjugated π-Spacer on Device Performance

Satyawan Nagane,‡[ab] Amol Ichake,‡[bc] Ishita Agrawal,[a] Aditya Sadhanala,[d] Richard H. Friend,[d]

Satishchandra Ogale*[a,e] and Prakash P. Wadgaonkar*[c]

Dedication ((optional))

Abstract: Three new D-A-π-A metal-free organic dyes *viz.* (*E*)-2-cyano-3-(10-dodecyl-7-(7-(10-dodecyl-10*H*-phenothiazin-3-yl)benzo[*c*][1,2,5]thiadiazol-4-yl)-10*H*-phenothiazin-3-yl)acrylic acid (**AI-1**), (*E*)-2-cyano-3-(10-dodecyl-7-(7-(10-dodecyl-10*H*-phenothiazin-3-yl)-2-octyl-2*H*-benzo[*d*][1,2,3]triazol-4-yl)-10*H*-phenothiazin-3-yl)acrylic acid (**AI-2**) and (*E*)-2-cyano-3-(10-dodecyl-7-(6-(10-dodecyl-10*H*-phenothiazin-3-yl)pyridin-2-yl)-10*H*-phenothiazin-3-yl)acrylic acid (**AI-3**) based on phenothiazine as donor and non-conjugated π-spacer were designed and synthesized. The incorporation of different 'internal acceptors' (electron traps) such as benzothiadiazole (BTD), benzotriazole (BTA) and pyridine were shown to allow systematic tuning of the energy levels and the photo-physical properties. **AI-1** dye showed lower electronic disorder as compared to the other two dyes. The efficiencies achieved with **AI-1**, **AI-2** and **AI-3** dyes were 8.5 % (Jsc = 15.42 mA/cm², Voc = 0.78 V, FF = 68 %), 7% (Jsc = 12.8 mA/cm², Voc = 0.78 V, FF = 68 %), and 6.7 % (Jsc = 11.57 mA/cm², Voc = 0.82 V, FF = 68.26 %), respectively. The incorporation of non- conjugated phenothiazine as a π-spacer in D-A-π-A dyes showed remarkable enhancement in photovoltaic performance of DSSC devices. The sealed DSSC devices with iodide/tri-iodide (I^-/I_3^-) based liquid electrolyte showed promising stability under ambient condition.

Introduction

The photovoltaic research has received significant attention after the discovery of dye sensitized solar cells (DSSCs) which have reached efficiencies up to 11-13 % using ruthenium-based metal dyes and porphyrin-based organic dyes.[1–3] However, these dyes face drawbacks such as poor thermal stability and tedious synthetic steps which are the major obstacles in their commercialization.[4] Therefore, the molecular engineering approach of organic dyes has captured great attention of researchers.[5] Towards this end, the attractive approaches involving donor–acceptor (D-A), acceptor-donor-acceptor (A-D-A) and donor–π-spacer–acceptor (D-π-A) based systems have been adopted and worked out.[6–11] D-π-A based systems have exhibited efficiencies of 9-10 %.[12–16] However, π-π stacking, inefficient electron injection and intermolecular recombination limit the photon conversion efficiency.[7,17,18] Thus, there is a need to fine tune these systems to overcome such problems. Hence, the engineering of molecular systems is needed to be taken into consideration. Zhu *et. al.* proposed D-A-π-A strategy for designing metal free organic sensitizers in which various internal acceptors such as BTD, BTA, quinoxaline etc. were incorporated.[19] The metal free organic D-A-π-A dyes achieved not only the broad band absorption but also photon conversion efficiencies upto 11-13%.[15,20,21]

Recently, Yang *et. al.* reported phenothiazine based D-π-A and D-A-π-A organic dyes for DSSCs. In the case of phenothiazine based dyes, D-A-π-A system with thiophene analogs as spacers afforded 6.4% power conversion efficiency.[22] The conjugated π-spacer in D-π-A dyes exhibited long range absorption but resulted in aggregation at TiO₂ surface which resulted in the decrease in J_{sc}, V_{oc} and FF.[23,24] Phenothiazine indeed acts as a strong donor having electron rich S- and N-hetero-atoms with non-planar butterfly conformation which helps in avoiding the molecular aggregation and intermolecular charge injection. The incorporation of phenothiazine into the molecular structure has several advantages over the other specified donors and π-spacers.[25–27] Therefore, we selected three different internal acceptors *viz.* BTD, BTA and pyridine which have different individual properties like strong acceptor, weak acceptor, or anchoring group, respectively, in the molecular structure.[28,29] These internal acceptor units are usually called as low band gap moieties which help in reducing the band gap of dyes and broaden their absorption spectra.[30] In this work, we have designed, synthesized and evaluated a new series of dyes based on D-A-π-A systems in which phenothiazine serves a dual role of donor as well as π-spacer.

[a]   S. Nagane, I. Agrawal, Prof. S. Ogale
       Centre of Excellence in Solar Energy, Physical and Materials
       Chemistry Division, CSIR-National Chemical Laboratory, Dr. Homi
       Bhabha road, Pashan, Pune, 411008. Maharashtra (India)
[b]   Academy of Scientific and Innovative Research (AcSIR),
       Anusandhan Bhawan, 2 Rafi Marg, New Delhi 110 001, India
[c]   A. Ichake, Dr. P. Wadgaonkar.
       Polymer Science and Engineering Division, CSIR- National
       Chemical Laboratory, Dr. Homi Bhabha Road, Pashan, Pune-
       411008, Maharashtra, India.
       E-mail: pp.wadgaonkar@ncl.res.in
[d]   Optoelectronics Group, Cavendish Laboratory, University of
       Cambridge, UK.
[e]   Prof. S. Ogale
       Department of Physics and Centre for Energy Science, Indian
       Institute of Science Education and Research (IISER), Dr. Homi
       Bhabha Road, Pune -411 008, Maharashtra, India.
       E-mail: satishogale@iiserpune.ac.in
[‡]   These authors contributed equally.
       Supporting information for this article is given via a link at the end of
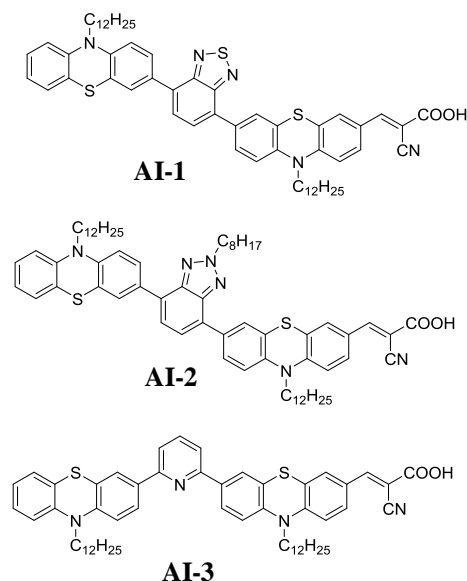   the document.((Please delete this text if not appropriate))

Figure 1. Structures of **AI** dyes.

Results and Discussion

Design and synthesis of AI dyes

The molecular engineering of the dyes (**Fig. 1**) was inspired by attractive properties of phenothiazine such as high electron donating ability and good opto-electronic properties.[24] **AI** dyes were synthesized by well known organic transformations.
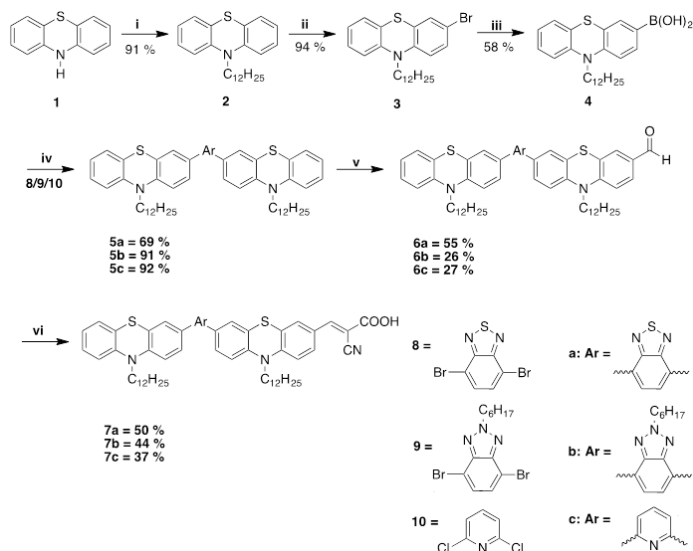
Reagents. i) KOH, KI, DMSO, n-$C_{12}H_{25}$Br, 80 °C; ii) NBS, DMF, 0 °C-rt; iii) n-BuLi, THF, triisopropyl borate -78 °C-rt; iv) Pd(PPh$_3$)$_4$, K_2CO_3, H_2O, THF, 80 °C; v) DMF, POCl$_3$, 1,2-dichloroethane, reflux; vi) cyanoacetic acid, piperidine, toluene, reflux.

Scheme 1. Synthesis of **AI** dyes.

In order to investigate the overall photovoltaic performance of synthesized dyes, we fabricated a set of dye sensitized solar cell (DSSC) devices. The photovoltaic performance of synthesized dyes was measured under AM 1.5 G illumination with I$^-$/I$_3^-$ as redox electrolyte and platinum coated FTO glass as a counter electrode. The commercially available dyesol TiO$_2$ paste was doctor bladed on cleaned FTO substrate to have mesoporous layer for dye to adsorb on.

Scheme 1 depicts a simple approach towards the synthesis of **AI-1**, **AI-2** and **AI-3** dyes containing phenothiazine as a donor and π-spacer moiety with different internal acceptors. N-alkylation of 10*H*-phenothiazine (**1**) was achieved using 1-bromododecane in the presence of potassium hydroxide as a base. N-alkylated phenothiazine intermediate (**2**) on bromination afforded bromo-phenothiazine (**3**). By using n-butyl lithium and triisopropyl borate, bromo-phenothiazine (**3**) was converted into boronic acid intermediate (**4**). Reaction between (**4**) and **8/9/10** by using Suzuki coupling afforded the desired compounds **5a-c**. The intermediate **6a-c** obtained by Vilsmeier-Haack formylation provided aldehyde intermediate which on Knoevenagel condensation with cyanoacetic acid yielded the target dyes **AI-1, AI-2** and **AI-3**.

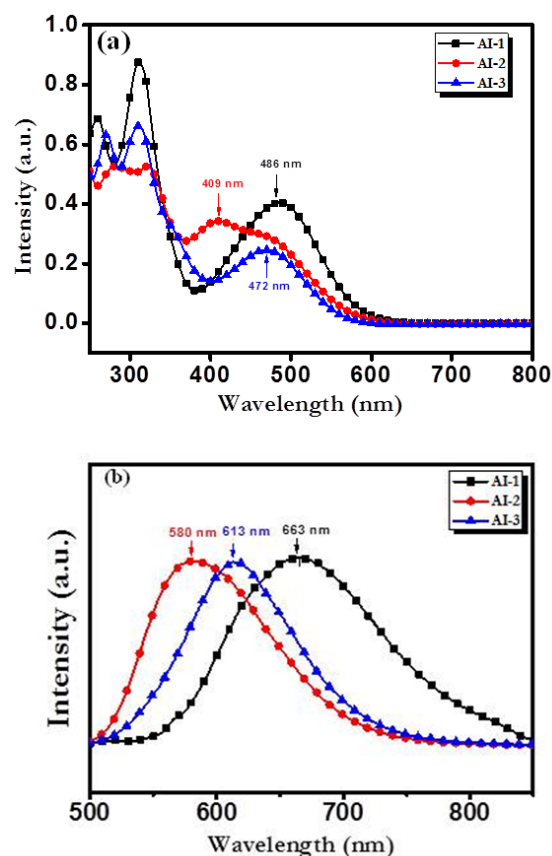### UV-Vis Absorption and photoluminescence properties

Figure 2. (a) UV-Vis absorption and (b) Photoluminescence spectra of **AI** dyes.

UV-Visible absorption spectra of **AI-1**, **AI-2** and **AI-3** dyes were shown in **Fig. 2 (a)**. These dyes exhibited strong absorption in UV and visible region with maximum absorption (λ_{max}) of 486 nm (ε = 24000 mol L^{-1} cm^{-1}), 474 nm (ε = 22000 mol L^{-1} cm^{-1}) and 472 nm (ε = 16000 mol L^{-1} cm^{-1}) for **AI-1**, **AI-2** and **AI-3,** respectively.

The systematic red shift was observed from **AI-3** to **AI-1**. The incorporation of BTD as strong internal acceptor in **AI-1** resulted in ~30 nm red shift as compared to **AI-2**. The pyridine based **AI-3** dye showed further blue shift in comparison with other synthesized dyes. Amongst the three dyes, **AI-1** showed broader absorption spectrum with higher molar extinction coefficient. The red shift in **AI-1** was attributed to the presence of sulfur containing heterocyclic BTD moiety as an internal acceptor. In the structure of BTA, the replacement of sulfur atom from BTD by C$_8$-alkylated nitrogen decreases its electron withdrawing character which has a significant impact on optical properties of **AI-2** dye. Interestingly, we observed marginal blue shift in absorption for **AI-3** dye which correlates with discontinuation in conjugation due to 2, 5 substitutions on pyridine moiety. The incorporation of non-conjugated phenothiazine as a π-spacer in **AI-3** showed ~20 nm red shift compared to reported **CMR401** in which phenothiazine was used as donor and pyridine as spacer without any particular π-spacer.[29] The multiple absorption peaks appeared in UV-spectra could be accounted to existence of different transitions in the molecules. The Density Functional Theory (DFT) calculations demonstrated that the band at 486 nm corresponds to HOMO-LUMO electron transition in **AI-1** dye.

Fig. 2(b) presents photoluminescence (PL) spectra of **AI-1**, **AI-2** and **AI-3** dyes. The PL measurements showed very broad emission which correspond to presence of internal acceptors into the dyes.[31] **AI-1** dye has showed emission maxima at 663 nm when the excitation wavelength is of 486 nm (which is a λ_{max} in optical absorption). When **AI-2** dye excited with its absorption maxima (409 nm), the emission occurs at 580 nm. In the case of **AI-3** dye, we observed emission at 613 nm after applying excitation wavelength of 472 nm. The nature of PL spectra depends on the presence of electron donating or withdrawing ability of these moieties in the dyes. Interestingly, **AI** dyes with three different electron acceptors having phenothiazine moieties at the adjacent positions showed systematic shift in PL spectra and gradual decrease in full width half maxima (FWHM). **AI-1** showed highest FWHM value of 138 nm which may be attributed to delayed fluorescence, as BTD moiety acts as strong electron trap.[32]

The incorporation of BTA in **AI-2** which is comparatively weaker electron acceptor than BTD showed lesser FWHM of 112 nm. In **AI-3**, pyridine showed weak acceptor amongst three dyes with FWHM of 100 nm. The presence
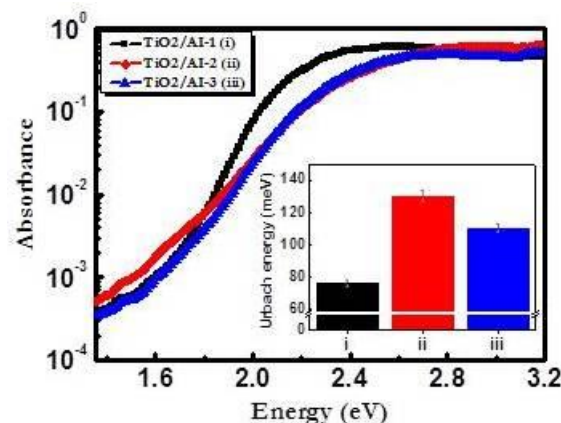

Figure 3. PDS spectra of **AI** dyes. Inset shows the Urbach energies for **AI** dyes as indicated.

of cyanoacrylic acid group at terminal position in dyes as electron withdrawing (anchoring) group may play major role in PL broadening.[33]

Photothermal deflection spectroscopy

Photothermal deflection spectroscopy (PDS) is a sensitive absorption measurement technique used to measure sub-band gap states and quantify the electronic disorder (in terms of Urbach energy) in a semiconductor.[34] Experimental details can be found elsewhere.[35] PDS spectra for all three dyes coated on quartz substrates were performed (**Fig. 3**). **AI-1** dye showed the steepest fall in the absorption below the band gap compared to **AI-2** and **AI-3**. These results in lower Urbach energies for the **AI-1** dye compared to **AI-2** and **AI-3** dyes that was reflected in the solar cell performances. **AI-1** dye based solar cells demonstrated the minimum Urbach energy and highest solar cells performance (as shown below) compared to **AI-2** and **AI-3** dyes. The Urbach energies of **AI-2** and **AI-3** have small differences but, are higher than **AI-1**, which reflected in their similar performance in solar cells (as shown below). The PDS (Fig. S1) and PL (Fig. 1b) spectra of the dyes made on quartz substrates showed a reverse trend between Urbach energy and PL FWHM indicating the different nature of electronic disorder experienced by absorptive and emissive species probed using PDS and PL, respectively.

Photo-excited electron dynamics for AI dyes

Fig. S2, (Supporting Information) showed PL lifetime decay of **AI-1**, **AI-2** and **AI-3** dyes in dichloromethane solution. PL decay measurements showed systematic enhancement in lifetime which is attributed to the electron withdrawing ability of individual internal acceptor. The alkyl substitution at

central nitrogen of BTA moiety in **AI-2** dye displayed its further advantage in electron lifetime measurements. **AI-3** dye showed highest life time of 9 ns in comparison with the other two dyes. The pyridine incorporation in dye structure allowed tuning of band energy levels in such a way that it could enhance the electron lifetime. **AI-1** dye showed sharp decay compared to other dyes. The observed lifetime for **AI-1**, **AI-2** and **AI-3** are 4 ns, 7 ns and 9 ns, respectively.
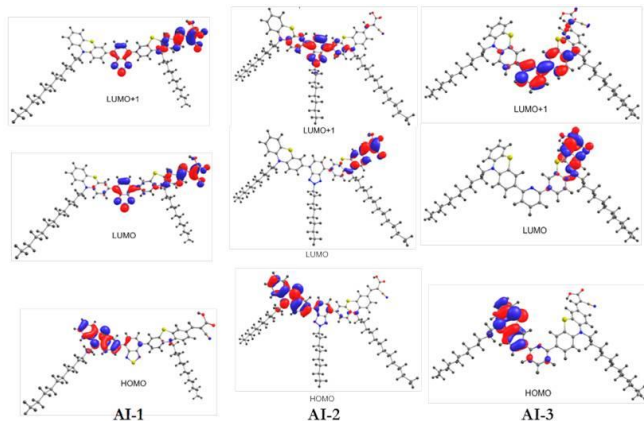

Figure 4. HOMO and LUMO of **AI** dyes calculated from DFT.

Electrochemical properties

We studied electrochemical properties of **AI-1**, **AI-2** and **AI-3** dyes by cyclic voltammetry (**Fig. S3**, Supporting Information). **Fig. S3** showed CV measurements of **AI-1**, **AI-2** and **AI-3** dyes in dilute solution of dichloromethane in the presence of tetrabutylammonium hexafluorophosphate as supporting electrolyte from which the information about redox nature of the dyes was extracted. The first oxidation potential corresponds to the HOMO level of dyes and reduction potential offers LUMO level of dyes. The HOMO levels were calculated using the oxidation potential value obtained from CV. The HOMO levels of **AI-1**, **AI-2** and **AI-3** were found to be -4.91eV, -4.88eV and -4.94eV, respectively with respect to vacuum level, and are more positive than the redox potential of I^-/I_3^- redox couple (-4.85eV). The incorporation of different internal acceptors in **AI** dyes showed slight shift in HOMO-LUMO level. The dyes showed appropriate band levels and were in good agreement with theoretical values which facilitate efficient charge transfer from the LUMO of dye to the conduction band of TiO_2.

Theoretical analysis

To examine the electronic properties and specific effect of incorporation of different internal acceptors in the dye molecules, we performed density functional theory (DFT) calculations using Gaussian 09 program at B3LYP/6-311G* level. The presence of two phenothiazine's (which has

butterfly like structure as shown in **Fig. 4**) and internal acceptors (BTD, BTA and pyridine) showed non-planarity in to the molecular structure which resulted in significant suppression of dye aggregation and internal charge recombination. For **AI-1**, **AI-2** and **AI-3** dyes, electronic distribution of the HOMO-LUMO are shown in **Figure 4**. DFT calculations demonstrated that HOMO in these dyes is mainly located on phenothiazine moieties. The observed electron density on donor phenothiazine is much higher compared to π-spacer phenothiazine in all cases that implies its specified role in dyes.

The LUMO level in **AI-1** dye lies on **BTD** and cyanoacrylic acid units. The LUMO situated on both the moieties can effectively separate the charges and inject into the conduction band of TiO_2 which resulted in higher J_{sc} and ultimately in the higher power conversion efficiency (PCE). On the other hand, the LUMO level of **AI-2** and **AI-3** dyes is mainly distributed on the cyanoacrylic acid moiety. The presence of auxiliary HOMO-LUMO levels such as LUMO+1 in dye molecules supports the existence of additional absorption bands in UV region.

Photovoltaic device performance

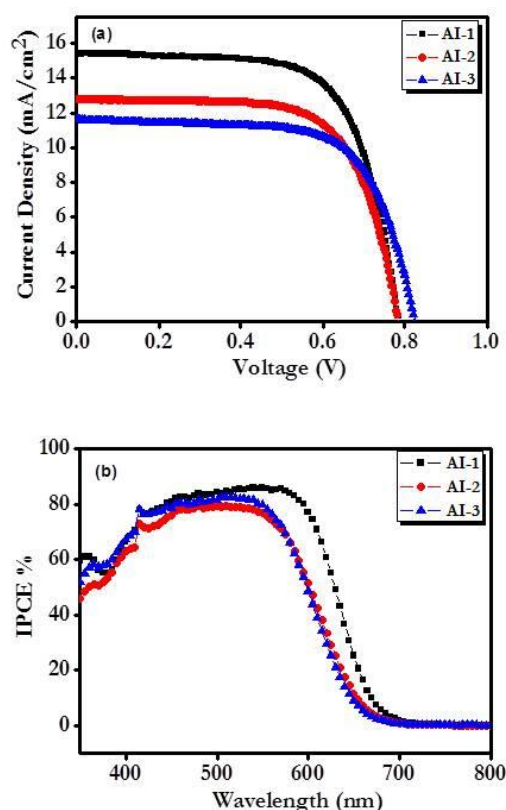We studied the effect of incorporation of internal acceptors

Figure 5. (a) J-V curves (b) IPCE of dyes **AI** with I^-/I_3^- redox electrolyte.

Table 1. Photovoltaic performance of **AI** dyes.

Dyes	J_{sc} (mA/cm^2)	V_{oc} (V)	Fill Factor (%)	Efficiency (η)
AI-1	15.42	0.78	68.0	8.5 ($\pm$0.3)
AI-2	12.8	0.78	68.0	7.0 ($\pm$0.1)
AI-3	11.57	0.82	68.26	6.7 ($\pm$0.1)

in the molecular structure of dyes. The influence of different internal acceptors on short circuit photocurrent (J_{sc}), photovoltage (V_{oc}), fill factor (FF) and power conversion efficiency (η) was investigated through the device characterization. We performed photovoltaic measurements of **AI** dyes with I^-/I_3^- electrolyte on 0.20 cm^2 active area. The **AI-1** dye showed efficiency of 8.5% (J_{sc} = 15.42 mA/cm^2, V_{oc} = 0.78 V, FF = 68%) with significant enhancement in J_{sc}. In case of **AI-2** and **AI-3** dyes, we achieved 7% (J_{sc} = 12.8 mA/cm^2, V_{oc} = 0.78 V, FF = 68%), and 6.7% (J_{sc} = 11.57 mA/cm^2, V_{oc} = 0.82 V, FF = 68.26%) of PCE with slight increment in V_{oc} but at same time linear decrease in J_{sc} values. **Fig. 5 (b)** showed incident photon conversion efficiency (IPCE) measurements of **AI-1**, **AI-2** and **AI-3** dyes. Interestingly, the IPCE of the **AI** dyes upto 500 nm were quite similar but after that substitution of strong electron withdrawing unit in **AI-1** dye showed red shift (25 nm) in visible region. **AI-2** and **AI-3** dyes showed marginal blue shift in IPCE spectra as compared to **AI-1** dye and it is clearly reflected in J_{sc} values. The incorporation of low band gap components instead of extended conjugated π-spacers improves the photo-stability of organic dyes and is able to facilitate charge transfer.[19] The electron deficient BTD unit acts as stronger internal acceptor compared to BTA.[30] In BTA, extra nitrogen at centre of benzo-fused five membered ring tuned molecular energy levels and alkyl chain on nitrogen may suppress the charge recombination.[36–39] Photovoltaic characterization showed significant enhancement in J_{sc}, V_{oc} and FF which indicated the reduction in overall charge recombination. For further
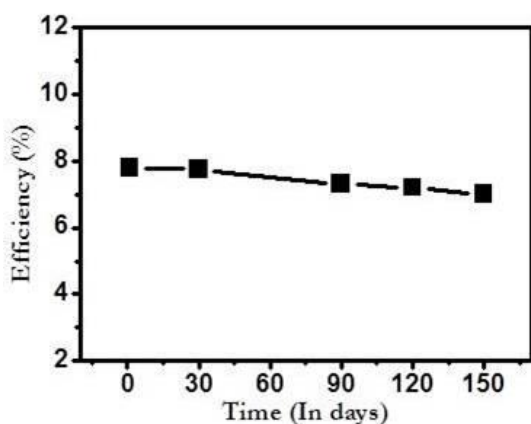
analysis, we carried out electrochemical impedance spectroscopy measurements to show the efficient interfacial charge transfer in **AI** dyes based solar cell devices (**Fig. S4**, Supporting Information).

The incorporation of pyridine into the molecular structure of dye offered well matching energy bands with TiO$_2$ and electrolyte. The favourable band alignment offered substantial reduction in fundamental losses such as dye regeneration and charge injection losses, which resulted in higher V_{oc} compared to **AI-1** and **AI-2** dyes. The lone pair of nitrogen in **AI-3** has ability to bind with oxygen vacancies of TiO$_2$ surface that could shift the Fermi energy level to lower binding energy. The band bending towards lower binding energy implies better charge transport.[26]

With these attractive performances of organic **AI** dyes as sensitizer in DSSCs, there is one crucial factor which needs to be addressed *viz.* stability. We performed photovoltaic measurements for six months to check the stability of devices under ambient conditions (**Fig. S5 and Table S1, Supporting information**). **AI-1** dye showed very high stability over 150 days (90% retention in solar cell device efficiency as displayed in **Fig. 6**) which is certainly a major advantage for large area solar cell devices.

Conclusions

In conclusion, we have designed, synthesized and characterized metal-free organic phenothiazine core D-A-π-A dyes based on three different internal acceptors viz. **BTD**, **BTA** and pyridine for DSSCs. The incorporation of different internal acceptors allowed to tune the energy bands and photo-physical properties systematically. The efficiencies achieved with **AI-1**, **AI-2** and **AI-3** dyes were 8.5%, 7.0% and 6.7%, respectively. The achieved efficiency of DSSC devices with iodine based liquid electrolyte showed promising stability and reproducibility. The designed D-A-π-A strategy with non-conjugated phenothiazine as π-spacer opens up tremendous opportunities for applications in large area solar cells. The incorporation **BTD** in the molecular structure showed lower electronic disorder which could be advantageously exploited in other opto-electronic applications.

Experimental Section

The experimental details are given in the supporting information, including the materials, device fabrication method, synthetic, photo-physical, electrochemical procedure and characterization of synthesized compounds.

Figure 6. Stability of **AI-1** dye.

Acknowledgements

[1] B. O'Regan, M. Gratzel, *Nature* **1991**, *353*, 737–740.
[2] M. K. Nazeeruddin, F. De Angelis, S. Fantacci, A. Selloni, G. Viscardi, P. Liska, S. Ito, B. Takeru, M. Grätzel, *J. Am. Chem. Soc.* **2005**, *127*, 16835–16847.
[3] A. Yella, H.-W. Lee, H. N. Tsao, C. Yi, A. K. Chandiran, M. K. Nazeeruddin, E. W.-G. Diau, C.-Y. Yeh, S. M. Zakeeruddin, M. Grätzel, *Science* **2011**, *334*, 629–634.
[4] D. Joly, L. Pelleja, S. Narbey, F. Oswald, J. Chiron, J. N. Clifford, E. Palomares, R. Demadrille, *Scientific Reports* 2014, *4*, 4033.
[5] W. Zhu, Y. Wu, S. Wang, W. Li, X. Li, J. Chen, Z.-S. Wang and H. Tian, *Adv. Funct. Mater.*, 2011, *21*, 756–763.
[6] W. Xu, B. Peng, J. Chen, M. Liang, F. Cai, *J. Phys. Chem. C* **2008**, *112*, 874–880.
[7] H. Tian, X. Yang, R. Chen, Y. Pan, L. Li, A. Hagfeldt, L. Sun, *Chem. Commun.* **2007**, 3741–3743.
[8] D. P. Hagberg, T. Marinado, K. M. Karlsson, K. Nonomura, P. Qin, G. Boschloo, T. Brinck, A. Hagfeldt, L. Sun, *J. Org. Chem.* **2007**, *72*, 9550–9556.
[9] N. Koumura, Z.-S. Wang, S. Mori, M. Miyashita, E. Suzuki, K. Hara, *J. Am. Chem. Soc.* **2006**, *128*, 14256–14257.
[10] W.-I. Hung, Y.-Y. Liao, C.-Y. Hsu, H.-H. Chou, T.-H. Lee, W.-S. Kao, J. T. Lin, *Chem. – Asian J.* **2014**, *9*, 357–366.
[11] S. S. Park, Y. S. Won, Y. C. Choi, J. H. Kim, *Energy Fuels* **2009**, *23*, 3732–3736.
[12] A. Mishra, M. K. R. Fischer, P. Bäuerle, *Angew. Chem. Int. Ed.* **2009**, *48*, 2474–2499.
[13] A. Hagfeldt, G. Boschloo, L. Sun, L. Kloo, H. Pettersson, *Chem. Rev.* **2010**, *110*, 6595–6663.
[14] M. Velusamy, K. R. Justin Thomas, J. T. Lin, Y.-C. Hsu, K.-C. Ho, *Org. Lett.* **2005**, *7*, 1899–1902.
[15] Z. Yao, M. Zhang, H. Wu, L. Yang, R. Li, P. Wang, *J. Am. Chem. Soc.* **2015**, *137*, 3799–3802.
[16] D. Joly, L. Pellejà, S. Narbey, F. Oswald, T. Meyer, Y. Kervella, P. Maldivi, J. N. Clifford, E. Palomares, R. Demadrille, *Energy Environ. Sci.* **2015**, *8*, 2010–2018.
[17] H. Lai, J. Hong, P. Liu, C. Yuan, Y. Li, Q. Fang, *RSC Adv.* **2012**, *2*, 2427–2432.
[18] M. Liang, J. Chen, *Chem. Soc. Rev.* **2013**, *42*, 3453–3488.
[19] Y. Wu, W. Zhu, *Chem. Soc. Rev.* **2013**, *42*, 2039–2058.
[20] N. Zhou, K. Prabakaran, B. Lee, S. H. Chang, B. Harutyunyan, P. Guo, M. R. Butler, A. Timalsina, M. J. Bedzyk, M. A. Ratner, et al., *J. Am. Chem. Soc.* **2015**, *137*, 4414–4423.
[21] Z. Yao, H. Wu, Y. Li, J. Wang, J. Zhang, M. Zhang, Y. Guo, P. Wang, *Energy Environ. Sci.* **2015**, *8*, 3192–3197.
[22] X. Yang, J. Zhao, L. Wang, J. Tian, L. Sun, *RSC Adv.* **2014**, *4*, 24377–24383.
[23] Z. Xie, A. Midya, K. P. Loh, S. Adams, D. J. Blackwood, J. Wang, X. Zhang, Z. Chen, *Prog. Photovolt. Res. Appl.* **2010**, *18*, 573–581.
[24] M. Marszalek, S. Nagane, A. Ichake, R. Humphry-Baker, V. Paul, S. M. Zakeeruddin, M. Grätzel, *J. Mater. Chem.* **2011**, *22*, 889–894.
[25] W. H. Nguyen, C. D. Bailie, J. Burschka, T. Moehl, M. Grätzel, M. D. McGehee, A. Sellinger, *Chem. Mater.* **2013**, *25*, 1519–1525.
[26] Y. J. Chang, P.-T. Chou, Y.-Z. Lin, M. Watanabe, C.-J. Yang, T.-M. Chin, T. J. Chow, *J. Mater. Chem.* **2012**, *22*, 21704–21712.
[27] Z.-S. Huang, H. Meier, D. Cao, *J. Mater. Chem. C* **2016**, *4*, 2404–2426.
[28] M. Göthelid, S. Yu, S. Ahmadi, C. Sun, M. Zuleta, M. Göthelid, S. Yu, S. Ahmadi, C. Sun, M. Zuleta, *Int. J. Photoenergy Int. J. Photoenergy* **2010**, *2011*, 2011, e401356.
[29] M. Cheng, X. Yang, J. Zhao, C. Chen, Q. Tan, F. Zhang, L. Sun, *ChemSusChem* **2013**, *6*, 2322–2329.
[30] D. G. (Dan) Patel, F. Feng, Y. Ohnishi, K. A. Abboud, S. Hirata, K. S. Schanze, J. R. Reynolds, *J. Am. Chem. Soc.* **2012**, *134*, 2599–2612.
[31] B. Gieseking, B. Jäck, E. Preis, S. Jung, M. Forster, U. Scherf, C. Deibel, V. Dyakonov, *Adv. Energy Mater.* **2012**, *2*, 1477–1482.
[32] L.-Y. Lin, Y.-H. Chen, Z.-Y. Huang, H.-W. Lin, S.-H. Chou, F. Lin, C.-W. Chen, Y.-H. Liu, K.-T. Wong, *J. Am. Chem. Soc.* **2011**, *133*, 15822–15825.
[33] H. Uoyama, K. Goushi, K. Shizu, H. Nomura, C. Adachi, *Nature* **2012**, *492*, 234–238.
[34] D. Venkateshvaran, M. Nikolka, A. Sadhanala, V. Lemaur, M. Zelazny, M. Kepa, M. Hurhangee, A. J. Kronemeijer, V. Pecunia, I. Nasrallah, et al., *Nature* **2014**, *515*, 384–388.
[35] A. Sadhanala, F. Deschler, T. H. Thomas, S. E. Dutton, K. C. Goedel, F. C. Hanusch, M. L. Lai, U. Steiner, T. Bein, P. Docampo, et al., *J. Phys. Chem. Lett.* **2014**, *5*, 2501–2505.
[36] Y. Wu, M. Marszalek, S. M. Zakeeruddin, Q. Zhang, H. Tian, M. Grätzel, W. Zhu, *Energy Environ. Sci.* **2012**, *5*, 8261–8272.
[37] J. N. Clifford, E. Martínez-Ferrero, E. Palomares, *J. Mater. Chem.* **2012**, *22*, 12415–12422.
[38] M. Zhang, J. Liu, Y. Wang, D. Zhou, P. Wang, *Chem. Sci.* **2011**, *2*, 1401–1406.
[39] Y.-S. Yen, C.-T. Lee, C.-Y. Hsu, H.-H. Chou, Y.-C. Chen, J. T. Lin, *Chem. – Asian J.* **2013**, *8*, 809–816.

FULL PAPER

Entry for the Table of Contents (Please choose one layout)

Layout 1:

FULL PAPER

Three new D-A-π-A metal-free organic dyes **AI-1**, **AI-2** and **AI-3** dyes showed efficiencies of **8.5 %** (J_{sc} = 15.42 mA/cm^2, V_{oc} = 0.78 V, FF = 68 %), **7%** (J_{sc} = 12.8 mA/cm^2, V_{oc} = 0.78 V, FF = 68 %), and **6.7 %** (J_{sc} = 11.57 mA/cm^2, V_{oc} = 0.82 V, FF = 68.26 %), respectively.
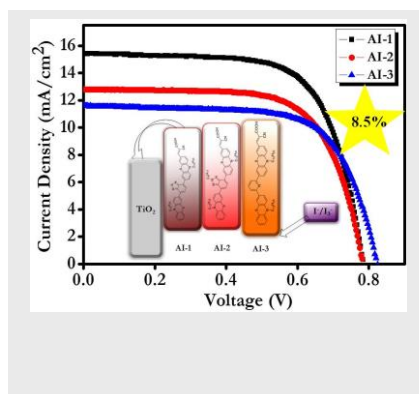
Satyawan Nagane,‡[ab] Amol Ichake,‡[bc]

Ishita Agrawal,[a] Aditya Sadhanala,[d]

Richard H. Friend,[d]

Satishchandra Ogale[a,e] and Prakash P.*

Wadgaonkar[c]*

Page No. – Page No.

Phenothiazine-Based D-A-π-A Dyes for Highly Efficient Dye Sensitized Solar Cells: Effect of Internal Acceptor and Non-Conjugated π-Spacer on Device Performance